Enhanced Fowler-Nordheim tunneling effect in nanocrystallite Si based LED with interfacial Si nano-pyramids

Gong-Ru Lin [1]*, Chun-Jung Lin[2], and Chi-Kuan Lin[2]

[1]Graduate Institute of Electro-Optical Engineering and Department of Electrical Engineering, National Taiwan University
No.1 Roosevelt Rd. Sec. 4, Taipei 106, Taiwan R.O.C.
[2]Department of Photonics and Institute of Electro-Optical Engineering, National Chiao Tung University
**Corresponding and Reprint Author E-mail: grlin@ntu.edu.tw*

Abstract: The premier observation on the enhanced light emission from such a metal-SiO_x-Si light emitting diode (MOSLED) with Si nano-pyramids at SiO_x/Si interface is demonstrated at low biases. The Si nano-pyramids exhibits capability in providing the roughness of the SiO_x/Si interface, and improving the Fowler-Nordheim (F-N) tunneling mechanism based carrier injection through the novel SiO_x/nano-Si-pyramid/Si structure. HRTEM analysis reveals a precisely controllable size and concentration of the crystallized interfacial Si nano-pyramids at 10nm(height)×10nm(width) and within the range of 10^8-10^{11} cm^{-2}, respectively. With these Si nano-pyramids at a surface density of up to $10^{12}/cm^2$, the F-N tunneling threshold can be reduce from 7 MV/cm to 1.4 MV/cm. The correlation between surface density of the interfacial Si nano-pyramids and the threshold F-N tunneling field has been elucidated. Such a turn-on reduction essentially provides a less damaged SiO_x/Si interface as the required bias for the electroluminescence of the MOSLED is greatly decreased, which thus suppresses the generation of structural damage related radiant defects under a lower biased condition and leads to a more stable near-infrared electroluminescence with a narrowing linewidth and an operating lifetime lengthened to >3 hours. An output EL power of nearly 150 nW under a biased voltage of 75 V and current density of 32 mA/cm^2 is reported for the first time.

OCIS codes: (230.3670) Light-emitting diodes; (250.5230) Photoluminescence; (310.1860) Deposition and fabrication

References and links

1. L. T. Canham, "Silicon quantum wire array fabrication by electrochemical and chemical dissolution of wafers," Appl. Phys. Lett. **57**, 1046-1048 (1993).
2. Q. Y. Ye, R. Tsu, and E. H. Nicollian, "Resonant tunneling via microcrystalline-silicon quantum confinement," Phys. Rev. B **44**, 1806-1811 (1991).
3. G. G. Qin, A. P. Li, B. R. Zhang, and B. C. Li, "Visible electroluminescence from semitransparent Au film/extra thin Si-rich silicon oxide film/p-Si structure," J. Appl. Phys. **78**, 2006-2009 (1995).
4. H. Z. Song, X. M. Bao, N. S. Li, and J. Y. Zhang, "Relation between electroluminescence and photoluminescence of Si^+-implanted SiO_2," J. Appl. Phys. **82**, 4028-4032 (1997).
5. C. H. Lin, S. C. Lee, and Y. F. Chen, "Strong room-temperature photoluminescence of hydrogenated amorphous silicon oxide and its correlation to porous silicon," Appl. Phys. Lett. **63**, 902-904 (1993).
6. L. Pavesi, L. Dal Negro, C. Mazzoleni, G. Franzo, and F. Priolo, "Optical gain in silicon nanocrystals," Nature **408**, 440-444 (2000).
7. F. Iacona, G. Franzo, and C. Spinella, "Correlation between luminescence and structural properties of Si nanocrystals," J. Appl. Phys. **87**, 1295-1303 (2000).

#77207 - $15.00 USD Received 17 November 2006; revised 26 January 2007; accepted 5 February 2007

8. G. Franzo, A. Irrera, E. C. Moreira, M. Miritello, F. Iacona, D. Sanfilippo, G. Di Stefano, P. G. Fallica, and F. Priolo, "Electroluminescence of silicon nanocrystals in MOS structures," Appl. Phys. A **74**, 1-5 (2002).
9. C.-J. Lin and G.-R. Lin, "Defect-enhanced visible electroluminescence of multi-energv silicon-implanted silicon dioxide film," IEEE J. Quantum Electronics **41**, 441-447 (2005).
10. G.-R. Lin, C.-J. Lin, C.-K. Lin, L.-J. Chou, and Y.-L. Chueh, "Oxygen defect and Si nanocrystal dependent white-light and near-infrared electroluminescence of Si-implanted and plasma-enhanced chemical-vapor deposition-grown Si-rich SiO_2," J. Appl. Phys. **97**, 094306 (2005).
11. R. H. Fowler and L. W. Nordheim, "Electron emission in intense electric fields," Proc. R. Soc. London, Ser. A **119**, 173 (1928).
12. S. S. Gong, M. E. Burnham, N. D. Theodore, and D. K. Schroder, "Evaluation of Q_{bd} for electrons tunneling from the Si/SiO_2 interface compared to electron tunneling from the poly-Si/SiO_2 interface," IEEE Trans. Electron Dev. **40**, 1251-1257 (1993).
13. K. V. Maydell, S. Brehme, N. H. Nickel, and W. Fuhs, "Electronic transport in P-doped laser-crystallized polycrystalline silicon," Thin Solid Films **487**, 93-96 (2005).
14. M. Ushiyama, Y. Ohji, T. Nishimoto, K. Komori, H. Murakoshi, H. Kume, and S. Tachi, "Two dimensionally inhomogeneous structure at gate electrode/gate insulator interface causing Fowler-Nordheim current deviation innonvolatile memory," IEEE Inr. Reliability Phys. Symp. **29**, 331-336 (1991).
15. T. Ohmi, M. Miyashita, M. Itano, T. Imaoka, I. Kawanabe, "Dependence of thin-oxide films quality on surface microroughness," IEEE Trans. Electron Dev. **39**, 537-545 (1992).
16. T. Sugino, C. Kimura, and T. Yamamoto, "Electron field emission from boron-nitride nanofilms," Appl. Phys. Lett. **80**, 3602-3604 (2002).
17. Y. P. Hsu, S. J. Chang, Y. K. Su, S. C. Chen, J. M. Tsai, W. C. Lai, C. H. Kuo, and C. S. Chang, "InGaN-GaN MQW LEDs with Si treatment," IEEE Photonics Tech. Lett. **17**, 1620-1622 (2005).
18. C.-L. Lee, S.-C. Lee, and W.-I. Lee, "Nonlithographic random masking and regrowth of GaN microhillocks to improve light-emitting diode efficiency," Jpn. J. Appl. Phys. **45**, L4-L7 (2006).

1. Introduction

Plasma enhanced chemical vapor deposition (PECVD) grown Si-rich SiO_2 or SiO_x with embedded Si nanocrystals (nc-Si) of extremely high density have been extensively investigated as a new class of light emitting material over decades [1-6]. To obtain room temperature electroluminescence (EL), both the metal/SiO_x/Si and the metal/n-Si/SiO_x/p-Si based light emitting diodes (LEDs) were demonstrated [7, 8], in which Fowler-Nordheim (F-N) and direct p-n junction barrier tunneling mechanisms were known to play important roles for the light emission from Si nanocrystals. However, the EL responses of such devices are usually not efficient due to the requirement of extremely high electric field for carriers tunneling through the insulating oxide channel [9, 10]. Therefore, versatile solutions have recently been developed to enhance the carrier injection efficiency, such as changing the contact metals, shrinking the optical bandgap, decreasing the barrier height, and reducing the resistivity of the host material, etc. In the work, we discuss the effect of PECVD grown nano-roughened SiO_x/Si interface on the enhancement of F-N tunneling in an indium tin oxide (ITO)/SiO_x/p-Si based metal-oxide-semiconductor light emitting diode (MOSLED). The surface density of roughened interfacial Si nano-pyramid structure and its correlation with the threshold electric field strength for initiating the F-N tunneling mechanism is determined.

2. Experimental

The Si-rich SiO_x film was deposited on *p*-type (100)-oriented Si substrate by PECVD at chamber pressure of 60 mtorr. The N_2O and SiH_4 fluences were controlled at 150 and 30 sccm, respectively, while the inductively couple plasma (ICP) power was varied from 60 to 30 watts. The Si substrate temperature was detuned between 200 and 400 ^oC during 5-min deposition. Typically, the sample was deposited at substrate temperature of 300^oC with an ICP power of 40-45 watts. To roughen the SiO_x/Si interface, the substrate temperature were raising up to 400 ^oC and the ICP power was decreasing to nearly threshold condition (25-30 watts), leading to the pre-deposition of randomized Si nano-pyramids on Si substrate prior to the growth of the SiO_x. To investigate the carrier transport, a 2000-Å ITO film layer (resistivity 33 Ω-cm) was deposited on the top of SiO_x with diameter of 0.8 mm to form the ITO/SiO_x/p-Si MOSLED. A 5000-Å Al contact was coated on the bottom of Si substrate

#77207 - $15.00 USD Received 17 November 2006; revised 26 January 2007; accepted 5 February 2007

following by an alloying process at 450 ^{o}C for 7.5 min.

3. Results and Discussion

3.1 Fowler-Nordheim Tunneling Enhanced Light Emission

First of all, the interface morphology of the PECVD grown SiO_x samples with different recipes was analyzed by high resolution transmission electron microscope (HRTEM) analysis, as shown in Fig. 1.

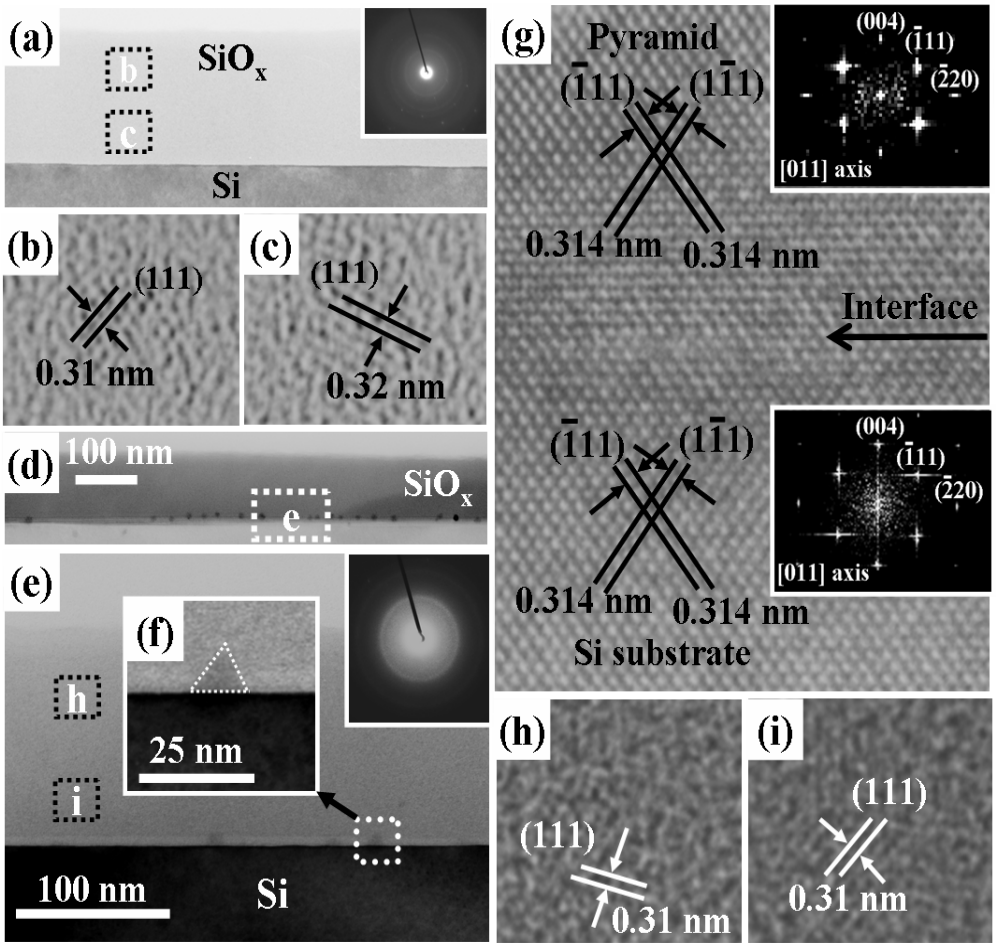

Fig. 1. Cross-sectional HRTEM photographs and corresponding electron diffraction patterns of Si-rich SiO_x grown at ICP powers of 45 (upper left) and 35 (lower left) watts. (a) The cross-sectional TEM photograph of the SiO_x film PECVD grown at normal ICP power. Inset: the electron diffraction pattern of the PECVD-grown SiO_x film. (b) and (c): the lattice parameter and orientation of the Si nanocrystals in PECVD-grown SiO_x film. (d) The cross-sectional TEM photograph of Si-rich SiO_x film with dense interfacial Si nano-pyramids grown at threshold ICP power. (e) The magnified cross-sectional TEM photograph of the Si-nano-pyramid embedded Si-rich SiO_x/Si interface. (f) The magnified TEM photograph for a single Si nano-pyramid and its electron diffraction pattern shown in the inset. (g): The observed orientations for the Si nano-pyramid (upper part) and Si substrate (lower part). (h) and (i): the orientation of the Si nanocrystals in the PECVD-grown Si-rich SiO_x film at threshold ICP-power condition.

For example, the cross-sectional view of the normally PECVD grown Si-rich SiO_x film shows smooth SiO_x/Si interface and precipitated Si nanocrystals with crystalline electron diffraction pattern. In contrast, the TEM photograph of the SiO_x sample grown at high

#77207 - $15.00 USD Received 17 November 2006; revised 26 January 2007; accepted 5 February 2007

substrate temperature and threshold ICP power further reveals the existence of dense Si nano-pyramids at the SiO_x/Si interface, while the interfacial Si nano-pyramid exhibits completely same electro diffraction pattern with that of the Si substrate. Under growing at the ICP powers of 35, 40, and 45 watts, the area densities of the interfacial Si nano-pyramids are estimated as 1.6×10^{11} cm^{-2}, 10^{9} cm^{-2}, and $<10^{8}$ cm^{-2}. Similar surface nano-pyramid density of 1.1×10^{11} cm^{-2} for the sample preparing at ICP power of 35 watts was also observed by AFM analysis. The Si nano-pyramids exhibit identical orientation with that of the Si substrate. The electric field (E) dependent emission current (I) can be described and the current-field plot can thus be fitted by F-N tunneling equations listed as below [11]:

$$I_{FN} = A_G A E^2 \exp(\frac{-B}{E}), \tag{1}$$

$$A = \frac{q^3 (m/m_{ox})}{8\pi h \Phi_B} = 1.54\times10^{-6} \frac{(m/m_{ox})}{\Phi_B} \left[\frac{A}{V^2}\right], \tag{2}$$

$$B = \frac{8\pi\sqrt{2m_{ox}\Phi_B^3}}{3qh} = 6.83\times10^7 \sqrt{(m_{ox}/m)\Phi_B^3} \left[\frac{V}{cm}\right], \tag{3}$$

where A_G is the gate area, E is the electric field, and A and B are usually considered to be constants. m_{ox} is the effective electron mass in the oxide, m is the free electron mass, and Φ_B is the effective barrier height. By linearly fitting the F-N plot of log (I/E^2) vs $1/E$, the F-N tunneling behavior can be confirmed according to the observation on the linear transferred function characteristic in the Arrhenius F-N plot, as shown in Fig. 2. The threshold electric fields to initiate F-N tunneling in three samples are ranging from 1.4 to 7 MV/cm, which indicates the effective potential barrier of the sample becomes smaller as the density of interfacial Si nano-pyramids increases. This essentially corroborates with the reduction on threshold electric field of F-N tunneling occurred in the sample grown at lower ICP powers.

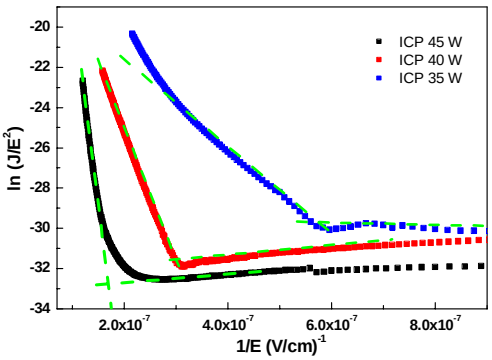

Fig. 2. The plots of ln(I/E^2) as a function of $1/E$ for three MOSLED samples with their SiO_x films PECVD grown at different ICP powers.

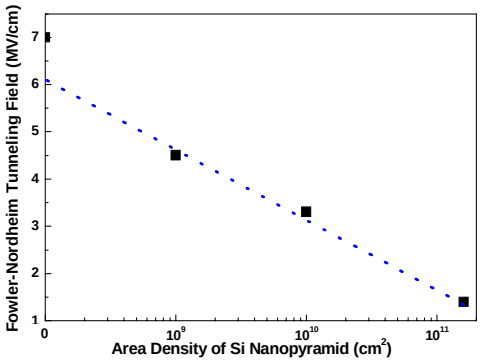

Fig. 3. Threshold F-N tunneling electric field as a function of the area density of Si nano-pyramids.

If we further illustrate the threshold F-N tunneling electric field as a function of the area density of Si nano-pyramids, a linear correlation can apparently be obtained and shown in Fig. 3. Obviously, the F-N tunneling mechanism has further been enhanced by increasing the area density of interfacial Si nano-pyramids. Due to the existence of Si nano-pyramids which behave like field emitters, the electrons will easily be gathered around the cone of the Si nano-pyramid and tunneled into the Si nanocrystals from the tip of the Si nano-pyramid, which consequently enhances the current injection and the electron-hole recombination. Similar phenomena have previously been observed in other material systems. Gong *et al.* [12] have observed that the roughness at the poly-Si/SiO_2 interface on both p- and n-well capacitors gives rise to higher electric fields and lower barrier heights and the breakdown degrades more with rising temperature. Maydell *et al.* [13] have investigated the electronic

#77207 - $15.00 USD Received 17 November 2006; revised 26 January 2007; accepted 5 February 2007

transport in laser-crystallized P-doped poly-Si, they concluded that the potential barrier height at the grain boundaries decreases with increasing electron concentration. This is due to a fact that the Fermi level in the grain may shift towards the band edge due to the doping, whereas the Fermi level at the grain boundary is pinned around the midgap due to the large amounts of dangling bonds on the poly-Si surface. Moreover, Ushiyama *et al*. [14] demonstrated with an atomic force microscope that the phosphorus-implanted poly-Si gate with an implanted dose below 10^{16} cm^{-2} and a low-temperature oxide annealing condition, could result in a smoother poly-Si/SiO_2 gate interface associated with a higher barrier. That is, the smooth interface with few defect are more resistant to the F-N tunneling process. Ohmi *et al*. [15] find the electric-field breakdown to be related to silicon surface micro-roughness, and Sugino *et al*. [16] have reported that the surface roughness effectively facilitates the reduction of the turn-on electric field and the effective potential barrier height, while the F-N tunneling based electron emission is enhanced by the boron-nitride nano-film with a more rough surface as compared to that of the Si substrate.

3.2 Performances of the Interfacial Si Pyramid based Si Nanocrystal MOSLED

Since the Si nano-pyramids also introduce the surface roughness on Si substrate, a large amount of the dangling bonds and associated defects could also exist at the SiO_x / Si interface. Under the large bias or high electric filed, the band structure of Si near the SiO_x/Si interface could be seriously bended, as shown in Fig. 4, where the charge distribution in the Si substrate would be inverted.

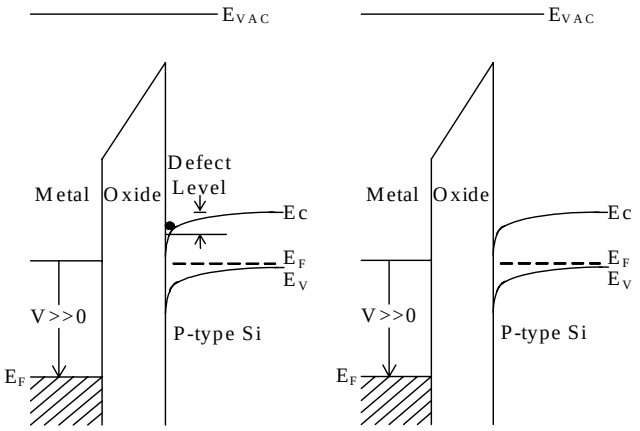

Fig. 4. The energy band diagrams of a highly biased MOSLEDs using SiO_x grown at different PECVD conditions. Left: the SiO_x grown at normal ICP power without Si nano-pyramids but with dense interfacial radiant defects. Right: the SiO_x grown at threshold ICP power with Si nano-pyramids at the SiO_x/Si interface.

With the increasing bias voltage, the energy level of the conduction band of Si will be lower than that of the defects distributed with the Si nano-pyramids, and the electrons trapped by these defects become free electrons. This also enhances the carrier transport and enlarges the tunneling current of the MOSLED at the same biased condition. In contrast, the band diagram of the sample without Si nano-pyramids shown in Fig. 4 is almost defect-free, in which the electrons (minority carriers) require a higher biased electric filed to tunnel through the barriers of the MOS structure. This also elucidates the significant reduction of threshold electric field and turn-on voltage of the ITO/SiO_x/p-Si/Al diode with interfacial Si nano-pyramids. The current-voltage (I-V) and current-optical power (I-P) characteristics of three ITO/SiO_x/p-Si/Al MOSLEDs with different densities of interfacial Si nano-pyramids are illustrated in Fig. 5.

#77207 - $15.00 USD Received 17 November 2006; revised 26 January 2007; accepted 5 February 2007

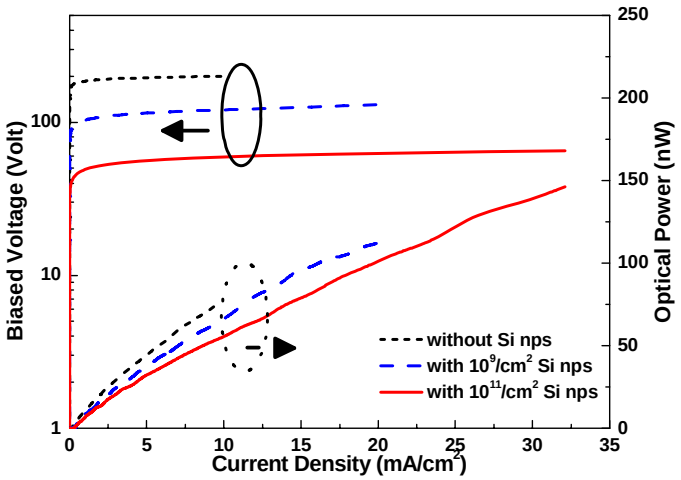

Fig. 5. The I-V and I-P curves of the ITO/SiO_x/p-Si/Al MOSLEDs with SiO_x films grown at different ICP powers. Upper: ICP power of 45 W. Middle: ICP power of 40 W. Lower: ICP power of 30 W.

It is clearly seen that both the smallest bias and the largest output power can be achieved if we reduce the ICP power of the PECVD system to facilitate the maximum growth of interfacial Si nano-pyramids. In particular, the EL power of the ITO/SiO_x/p-Si/Al MOSLED with the highest Si nano-pyramid density can be enlarged by two times as compared to that of the similar device without any interfacial Si nano-pyramids. From HRTEM analysis for the annealed SiO_x film with and without interfacial Si nano-pyramids, as shown in Fig. 6. The densities of nc-Si within the SiO_x grown without and with interfacial Si nano-pyramids are 5.7 × 10^{18} cm^{-3} (left part of Fig. 6) and 3.7 × 10^{19} cm^{-3} (right part of Fig. 6). It is thus corroborated that the density of nc-Si embedded in SiO_x significantly decreases as the interfacial Si nano-pyramids occurs. Therefore, the slope efficiency of the ITO/SiO_x/p-Si/Al MOSLED with interfacial Si nano-pyramids is inevitably reduced as the buried nc-Si dilutes (see Fig. 5). The EL spectra of ITO/SiO_x/p-Si/Al MOSLEDs with and without interfacial Si nano-pyramids biased at maximum output condition are compared, as shown in Fig. 7.

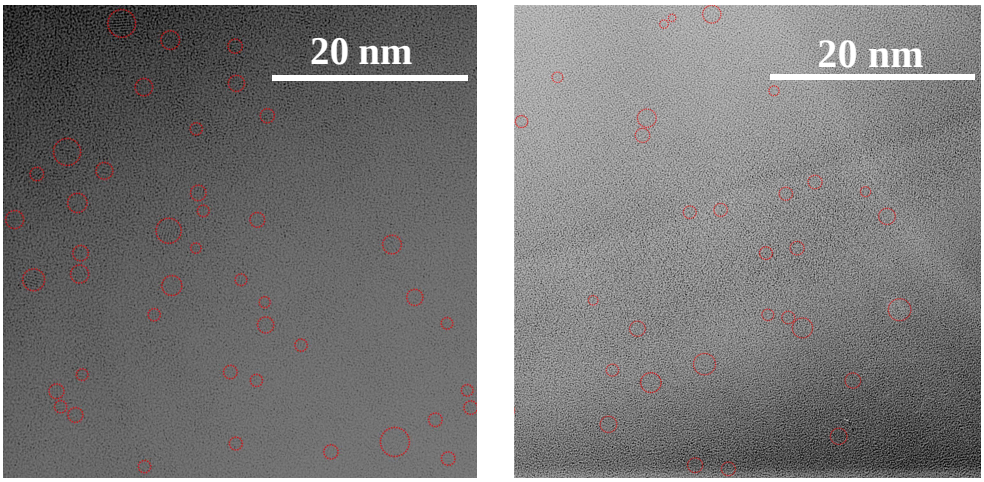

Fig. 6. TEM images of nc-Si within the annealed SiO_x film grown without (left) and with (right) interfacial Si nano-pyramids.

For the MOSLED samples without interfacial Si nano-pyramids, the nc-Si related near-infrared EL with dual peaks at 455 and 740 nm is observable at biased voltage larger than

#77207 - $15.00 USD Received 17 November 2006; revised 26 January 2007; accepted 5 February 2007

160 V. The nc-Si dependent EL component slightly blue-shifts from 740 to 690 nm as the biased voltage increases from to 160 V to 200V, whereas the blue-green EL peak wavelengths remain unchanged. Such a blue-shifted near-infrared EL peak clearly indicates different luminescent mechanisms occurred as the band bending becomes serious under an extremely high electric field, leading to the carriers between adjacent nc-Si tunneled from first-order quantized state (n=1) to second-order quantized state (n=2).[10] In addition, the unanticipated EL peaks at central wavelength of 455 nm also grows up with increasing biases, which are contributed by oxygen dependent structural defects such as the neutral oxygen vacancy (NOV) centers[4] generated in the oxide layer when biased at nearly breakdown condition. Alternatively, the ITO/SiO_x/p-Si/Al MOSLED with interfacial Si nano-pyramids biased at 70 V reveals an EL spectra with smaller defect-dependent emissions. The nc-Si dependent broad spectra ranging between 650 and 850 nm is not shifted with the increasing bias. The operation of a MOSLED at such a lower electric field could not contribute to serious band bending, thus avoiding the cold-carrier tunneling process happened between adjacent nc-Si. In this case, the blue-shifted near-infrared EL phenomenon no longer exists on the Si nano-pyramid enhanced MOSLED device. Furthermore, the lower electric field required for the EL under the assistance of interfacial Si nano-pyramids prevent the generation of structural damage as well as the corresponding NOV defects, thus attenuating the defect related EL at blue-green region as compared to the typical MOSLED without interfacial Si nano-pyramids.

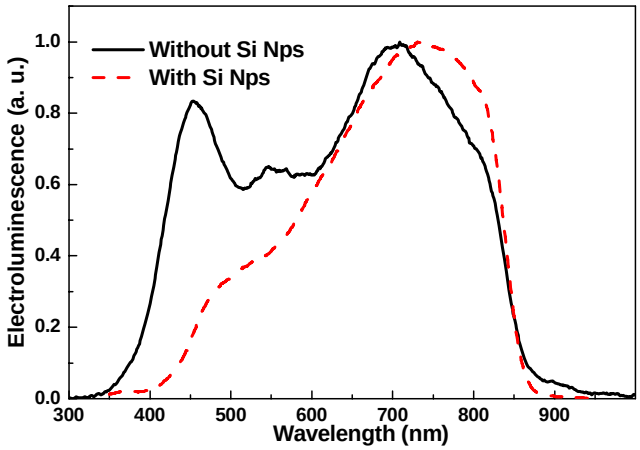

Fig. 7. EL spectra of ITO/SiO_x/p-Si/Al MOSLEDs with (solid) or without (dashed) interfacial Si nano-pyramids.

For comparison, all of the key device parameters of the samples grown at different ICP powers were listed in Table I. These oxygen correlated interfacial states play dominant roles on the white-light emission from ITO/SiO_x/p-Si/Al MOSLED at the high electrical field, which are unstable as a highly biased condition is required to trigger the defect-enhanced EL. The bias dependent surface-emitting EL patterns of a diode made on the Si-rich SiO_x with and without interfacial Si nano-pyramids are shown in Fig. 8. Larger EL power obtained for the typical ITO/SiO_x/p-Si/Al MOSLED without Si nano-pyramids is partially attributed to the radiant defects generated in damaged SiO_x structure operated under such a nearly breakdown condition ($E_{breakdown} \approx 10$ MV/cm). The radiative defects usually contribute to a broadened EL at shorter wavelength region, which inevitably results in an EL pattern with a bright color (see upper row in Fig. 8).

#77207 - $15.00 USD Received 17 November 2006; revised 26 January 2007; accepted 5 February 2007

Table I. Key parameters of the MOSLEDs with interfacial Si nano-pyramids (Si-nps) of different densities.

Parameters	S1	S2	S3
Si-nps Area Density (cm^{-2})	0	10^9	1.6×10^{11}
$E_{F\text{-}N\ threshold}$ (V/cm)	7×10^6	3.2×10^6	1.4×10^6
$V_{turn\text{-}on}$ (V)	187	105	50
$I_{turn\text{-}on}$ (mA/cm^2)	1.5	0.25	0.1
P_{max} (nW)	9	20	150
P-I slope (mA/W)	0.75	3	5.2
$\eta_{external\ efficiency}$ (%)	6.6×10^{-5}	5.8×10^{-4}	2.1×10^{-3}

Although the ITO/SiO_x/p-Si/Al MOSLED with interfacial Si nano-pyramids can not reach the same EL power as compared to those without Si nano-pyramids at same biased condition, which is still able to emit larger EL power at higher current and lower biased conditions. In contrast to the conventional MOSLEDs operated at biases nearly breakdown, the interfacial Si nano-pyramids also behaves like tipped field emitters to release breakdown of the MOSLEDs. On the other hand, a release on the critical emitting angle which is needed to avoid total internal reflection (TIR) has also been considered in previous studies of the LEDs [17, 18], which facilitates a larger fraction of light emitted from the active region of LED. Versatile methods of surface roughening have been introduced to improve the external quantum efficiency of LEDs. In our results, the interfacial Si nano-pyramids on the surface of Si substrate also acts like a novel surface roughened layer, which not only enlarge the current injection by enhancing F-N tunneling in the ITO/SiO_x/p-Si/Al MOSLED, but also improve the external quantum efficiency of light emission by releasing the critical TIR angle limitation with the roughened SiO_x/Si interface. Consequently, the external quantum efficiency and the maximum EL output power of the ITO/SiO_x/p-Si/Al MOSLED with interfacial Si nano-pyramids can be increasing at a lower biased condition, as shown in Fig. 5.

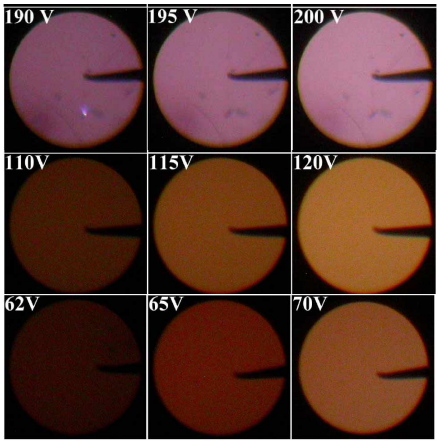

Fig. 8. Far-field EL patterns of three MOSLED samples without (upper) and with Si-nano-pyramid concentrations of $\rho=10^9/cm^2$ (middle) and $\rho=10^{11}/cm^2$ (lower).

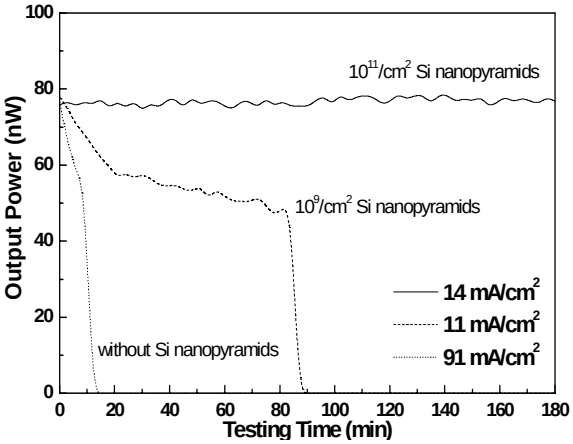

Fig. 9. Output power stability of three MOSLED samples with different Si-nano-pyramid concentrations.

If we further characterize the lifetime for three different samples, it is clearly seen that the typical device without Si nano-pyramids will be damaged within 10 minutes even operating at below breakdown condition, as shown in Fig. 9. The lifetime of the MOSLED device can be effectively lengthened to several hours by introducing the Si nano-pyramids which reduces the

#77207 - $15.00 USD Received 17 November 2006; revised 26 January 2007; accepted 5 February 2007

biased field away from the breakdown. The radiant defects although contributes the EL power, however, which also degrade the lifetime performance of the MOSLED device. Our experimental results have interpreted the importance of PECVD growing condition on the synthesis of Si nano-pyramids, which rely on adjusting a large desorption rate of the SiH_4 under a oxygen-deficient environment, following by the deposition of the defect-free Si-rich SiO_x film at high substrate temperature and threshold ICP power condition. In comparison, the growth condition of lower substrate temperature and higher ICP power inevitably contribute to a faster deposition rate with smaller excess Si density under an oxygen-rich environment, which degrades the precipitation of the interfacial Si nano-pyramids and fails to enhance the carrier transport in the diode.

4. Conclusions

In conclusion, the premier observation on the enhanced F-N tunneling mechanism from the novel SiO_x/nano-Si-pyramid/Si structure is demonstrated. Dense Si nano-pyramids can be synthesized at the SiO_x/Si interface by reducing the ICP power during the PECVD growth of Si-rich SiO_x on Si with high substrate temperature. The correlation between the surface density of interfacial Si nano-pyramids and the threshold F-N tunneling field has been illustrated. With these interfacial Si nano-pyramids at a surface density of 1.6×10^{11} cm^2, the F-N threshold can be reduced from 7 to 1.4 MV/cm. The elucidation on the role of the Si nano-pyramids played on the improved carrier transport and enhanced light emission properties are addressed. The existence of Si nano-pyramids greatly reduces the biased voltage from 200 to 65 V, which is required to obtain sufficient EL power from the MOSLEDs. Consequently, a more stable near-infrared electroluminescence is emitted from the ITO/SiO_x/p-Si/Al MOSLED with interfacial Si nano-pyramids, providing a narrowing linewidth and a lengthened lifetime to >3 hours at room temperature operation. To date, an output EL power of nearly 150 nW under a biased voltage of 75 V and current density of 32 mA/cm^2 is reported.

Acknowledgments

This work was supported in part by National Science Council (NSC) of Taiwan, Republic of China, under grants NSC94-2215-E-002-054, NSC94-2120-M-002-010, and NSC95-2221-E-002-448.

#77207 - $15.00 USD Received 17 November 2006; revised 26 January 2007; accepted 5 February 2007